This document was prepared in conjunction with work accomplished under Contract No. DE-AC09-96SR18500 with the U. S. Department of Energy.

ANALYTICAL MODEL FOR PREDICTION OF PLATE-SPECIFIC FRACTURE TOUGHNESS PROPERTIES OF ASTM A285 STEEL

K. H. Subramanian, B. J. Wiersma, A. J. Duncan, S. P. Harris
Savannah River Technology Center
Westinghouse Savannah River Company
Aiken, SC USA

ABSTRACT

A materials test program was developed to measure mechanical properties of A285 carbon steel under conditions relevant to waste storage tanks at the Savannah River Site. Fracture toughness and tensile testing were performed on ASTM Type A285 steels that span tank plate compositions. Variables relevant to the material and load conditions for Type I and Type II tanks were defined and a statistical test matrix was designed for fracture toughness testing. The test matrix consisted of eight variables expected to influence mechanical properties. The independent variables were carbon content, manganese content, sulfur content, thickness, pearlite fraction, and grain size. The responses were the fracture toughness J_{Ic}, and a figure-of-merit at J_{3mm} to allow for sub-critical ductile crack growth. A total of 85 J-R curves were compiled, of which 29 were tests done at a quasi-static rate in the T-L orientation, 29 were done at a quasi-static rate in the L-T orientation, 15 were done at a dynamic rate in the T-L orientation, and 12 were done at a dynamic rate in the L-T orientation. The full data set was used to construct analytical models to predict fracture properties as a function of material properties and operating conditions. Eight independent models resulting from combinations of loading rate (quasi-static, dynamic) and orientation (T-L, L-T) were developed. The statistical significance of terms was determined for each of the models. Thickness and grain size were found to be of statistical significance in the models developed for the dynamic strain rate testing data. Compositional variables were found to be of statistical significance for the quasi-static loading rate fracture toughness data.

INTRODUCTION

A structural integrity program is in place to ensure structural adequacy of storage tanks at the Department of Energy (DOE)-Savannah River Site (SRS) . As part of the structural integrity program, fracture mechanics analysis is done to ensure the flaw tolerance of the tanks. Fracture mechanics analysis can be used to determine the critical crack size that can lead to unstable ductile tearing conditions. The validity and limitations of the fracture mechanics analysis depend, in part, upon the available mechanical property data applicable to the material of construction (ASTM A285 Grade B steel).

Mechanical properties have previously been compiled for ASTM A285 Grade B steel for elastic-plastic fracture mechanics analysis of the waste storage tanks [1]. The properties were compiled from Charpy V-Notch (CVN), 0.4T planform compact tension (C(T)), and tensile specimens from archival steel scavenged from large water piping. The influence of material composition, temperature, geometry, and loading rates were presented based upon the initial database. The study recommended that a database be developed to quantify the role of these variables on the fracture toughness. As a result, a mechanical testing program was developed to provide input to a model that can calculate a statistically based estimate of fracture toughness properties for flaw specific structural analysis. The materials properties will be used to perform J_R

analysis or develop failure assessment diagrams (FAD) to evaluate structural integrity.

The minimum operating temperature of the storage tanks is 70°F (21°C) placing the carbon steel in the upper transition region where ductile tearing is expected to be the primary failure mode[2]. Elastic-plastic analysis must be used to characterize the deformation of the thin wall tanks (0.5”–0.875”). The approach of using EPFM allows determination of critical flaw size under conditions where stable crack extension precedes instability.

MATERIALS

The carbon steel material for the waste storage tanks was fabricated per specification ASTM A285-50T, Grade B firebox quality (A285) [3]. The nominal composition of ASTM A285 steel is shown in Table 1. Available material of current vintage was selected to closely match the materials used in the storage tanks. The materials selected for testing were chosen based on their representative levels of carbon, manganese, phosphorus and sulfur as shown in Table 2.

Table 1: ASTM Requirements for Chemical Composition for A285-50T, Grade B Firebox Quality

For plates ≤ 0.75” thickness	**Composition, %**			
	C_{max}	**Mn_{max}**	**P_{max}**	**S_{max}**
	0.2*	0.8	0.035	0.04

*C = 0.22 wt.% for plate of 0.75”< thickness ≤ 2”

Statistical Test Matrix

Variables relevant to the material and load conditions for the waste storage tanks were defined and a statistical test matrix was designed for fracture toughness testing. The test matrix consisted of six independent variables (shown in Table 2) that were expected to influence mechanical properties. Eight independent models resulting from combinations of loading rates (quasi-static, dynamic) and orientations (T-L, L-T) were developed.

Table 2: Test Matrix Variable Description

Variable	**Span**	
C Content	0.08 wt%	0.23 wt%
Mn Content	0.35 wt%	0.9 wt%
S Content	0.005 wt%	0.04 wt%
Thickness	0.5"	0.875"
Loading Rate*	Quasi-static	Dynamic
Orientation*	L-T	T-L

Heats Tested

Heats of steel were chosen for testing based upon tank construction materials, but limited by availability. The 10 heats chosen for testing, plate thickness, chemical composition and tensile properties are listed in Table 3 and Table 4. All these heats meet the Grade C specification. Heat "Adisk" represents archival steel found at the SRS without materials certification. These heats were produced of semi-killed steel and hot rolled to the indicated plate thickness shown. On-site compositional analysis determined that the carbon, manganese, and sulfur content were similar to ASTM A285 specifications. The archival material provided insight into variation between older vintage steels and the heats of steel that were machined from newer steel plates. Interim observations on data subsets revealed that higher loading rates lead to more rapidly increasing J-curves in recent vintage low-carbon steels in comparison with quasi-static loading rates. However, for archival material, containing higher carbon contents, the effect is less pronounced [4].

Table 3: Composition of the Heats

Heat #	**Plate Thick. (in.)**	**C Wt%**	**Mn Wt%**	**S Wt%**
1A5864	0.5	0.097	0.432	0.014
1A664	0.5	0.063	0.484	0.015
1A434	0.875	0.082	0.676	0.011
A3184	0.625	0.1	0.86	0.013
K325	0.75	0.11	0.86	0.006
395331	0.5	0.1	0.83	0.005
Adisk	1.125	0.23‡	0.42‡	0.027‡
7463960	1.0	0.18	0.82	0.01
E400	0.625	0.18	0.43	0.026
P134	1.125	0.083	0.854	0.032

Table 4: Tensile Properties of Tested Heats

Heat #	**s_y**	**s_{UTS}**	**Elong.****

	(ksi)	(ksi)	(%)
1A5864	44.0	62.0	30
1A664	44.0	61.0	32
1A434	46.0	64.0	28†
A3184	41.4	60.1	29
K325	50	64	26
395331	45.8	66.5	30
Adisk	33.9⁺	65.2⁺	37.4⁺
7463960	43.0	66.0	29
E400	42	62	28
P134	40.0	60.0	35†

*from the manufacturers' materials test certificates unless noted
**All values are for an 8 inch gage length except when noted
† 2 inch gage length
‡ from on-site chemical analysis
⁺ from tensile tests performed on the actual plate on 1in. gage samples

Metallography

The microstructure of ASTM A285 steel consists of ferrite and pearlite. Metallography revealed banding of the pearlite in the T-L and the L-T orientations. The banding is due to the microsegregation of manganese, non-metallic inclusions, and the hot-rolling finishing temperature/cooling rate. The banding concentration can be altered by heat treatment. Furnace cooled conditions lead to a banded structure, while air-cooled structures have been found to yield no banding [5].

The mechanical properties of ferrite/pearlite steel are dependent upon several microstructural features, including the grain size and the volume fraction of pearlite. Table 5 contains the grain sizes and the volume fraction of pearlite for the steels tested. As grain size increases, the impact transition temperature is increased and the yield stress is slightly reduced. Pearlite influences fracture because it work-hardens more rapidly than the ferrite, and is thus more likely to initiate a brittle crack. The mechanism of failure in the pearlite is dependent upon interlamellar spacing, the orientation of the pearlite with respect to the stressing direction, and the strain rate [6]. Once the crack is initiated, the crack must grow through the ductile ferrite matrix. The crack growth is dependent upon void nucleation and coalescence in the ferrite matrix.

Table 5: Metallographic Analysis of Steel Heats Tested

Heat	Grain Size (μm)	V_f (pearlite)
1A5864	46	10
1A664	47	10
1A434	52	11
A3184	48	13
K325	55	12
395331	47	12
Adisk	55	17.5
7463960	51	16
E400	51	16
P134	52	11

FRACTURE TOUGHNESS TESTING

The standard method for J-integral characterization described in ASTM Standard E1820: "Standard Test Method for Measurement of Fracture Toughness" was followed to develop J-R curves [7]. Fracture toughness tests were conducted on compact tension specimens (C(T)) machined to ASTM E1820 specifications (shown in Figure 1), with the exception of a large uncracked ligament 'W', to allow for back end constraint and for measurement of fracture energy 'J' at large crack extensions. The specimens were side-grooved to prevent extensive crack tunneling. The specimens were fatigue-precracked according to ASTM E1820 specifications. The quasi-static and dynamic loading rates (load-line displacement rates) were 1.24×10^{-4} in/sec and 0.11 in/sec respectively. The quasi-static rate translates to a stress intensity of 0.667 ksi-in$^{1/2}$/min. The dynamic rate is based upon the response of the structure to a seismic event.

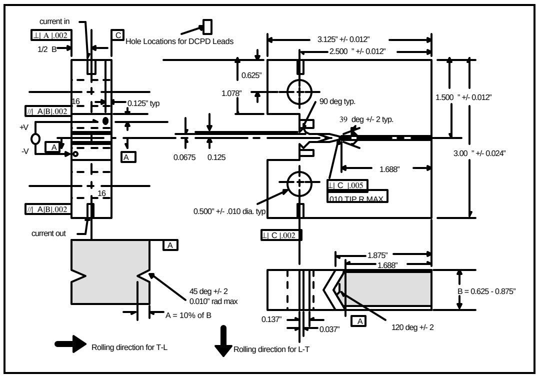

Figure 1: Compact Tension Specimen Design

Fracture toughness testing was performed on a MTS hydraulic load frame in a temperature controlled test chamber (shown in Figure 2). Load, load-line displacement and crack lengths were measured for calculation of J-Δa curves. Load-line displacement was measured through the MTS controller to allow for extensive crack opening during testing.

Figure 2: Specimen Setup in Test Chamber with Crack Length Potential Drop Measurement System

Two critical points of fracture energy, J, were chosen for model development: (1) J_{Ic} (per ASTM E1820) and (2) a J_{3mm} figure-of-merit. The figure-of-merit of J at 3 mm of crack extension was selected to allow for sub-critical crack growth, even at the dynamic strain rate. The values for J_{3mm} were determined using a power law fit as constructed in ASTM E1820. A total of 85 J-R curves were compiled, of which 29 were tests done at the static rate with the T-L orientation, 29 were done at the static rate in the L-T orientation, 15 were done at the dynamic rate in the T-L orientation, and 12 were done at the dynamic rate in the L-T orientation. . The full data set was used to construct analytical models capable of predicting J_{Ic} and J_{3mm} fracture properties. Eight independent models resulting from combinations of loading rate (static, dynamic), orientation (T-L, L-T) for J_{Ic} and J_{3mm} were developed.

RESULTS

The data, J_{Ic} and J_{3mm} values, for each orientation and loading rate combination are shown in Figures 3-12. The loading rate, orientation, and thickness shown are specific to the specimen. The carbon, manganese, and sulfur content are heat-specific. Subsets of data have previously been presented with preliminary observations [8].

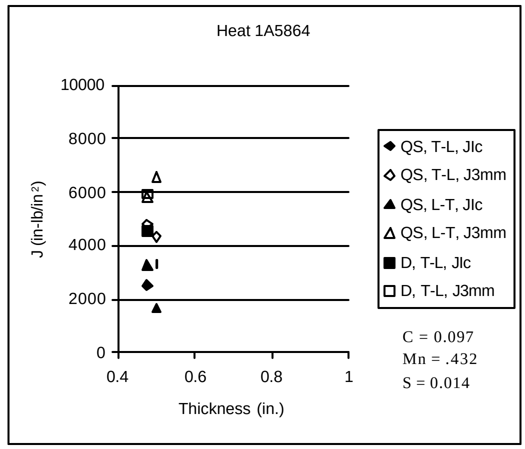

Figure 3: Fracture Toughness Response of Heat 1A5864

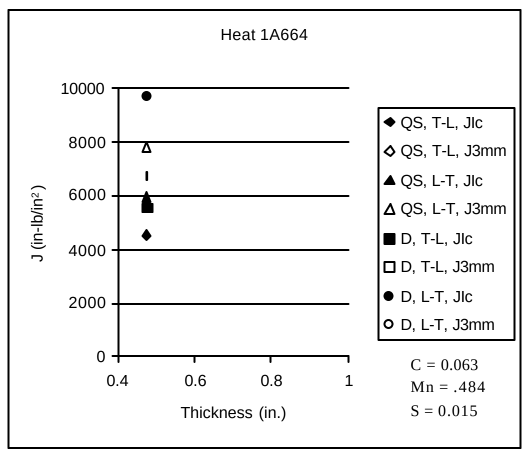

Figure 4: Fracture Toughness Response of Heat 1A664

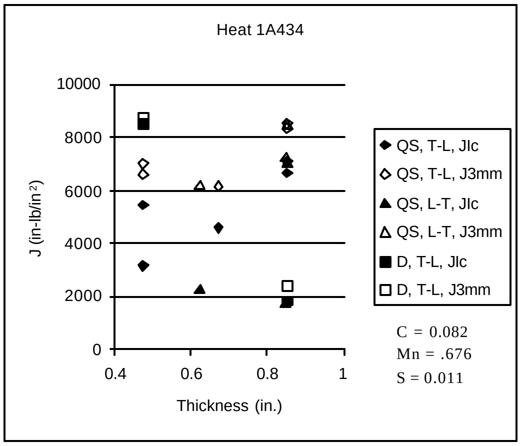

Figure 5: Fracture Toughness Response of Heat 1A434

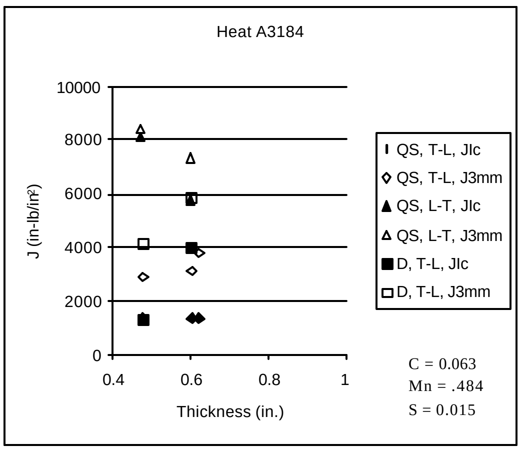

Figure 6: Fracture Toughness Response of Heat A3184

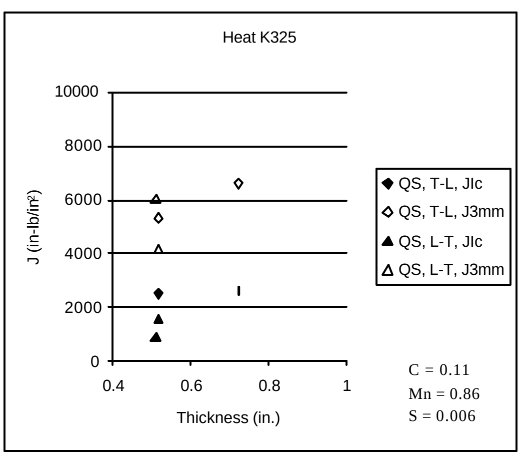

Figure 7: Fracture Toughness Response of Heat K325

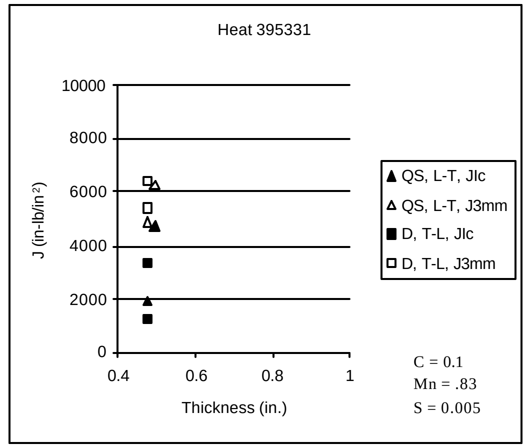

Figure 8: Fracture Toughness Response of Heat 395331

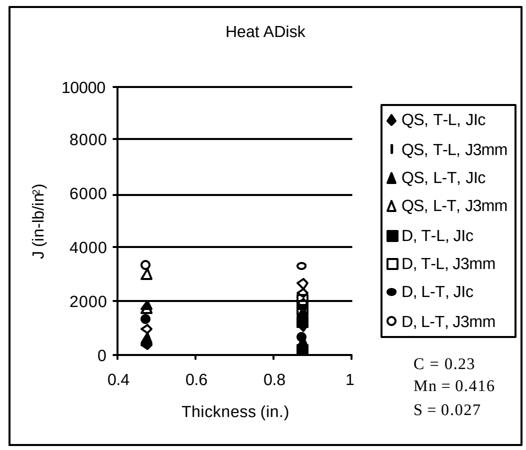

Figure 9: Fracture Toughness Response of Heat Adisk

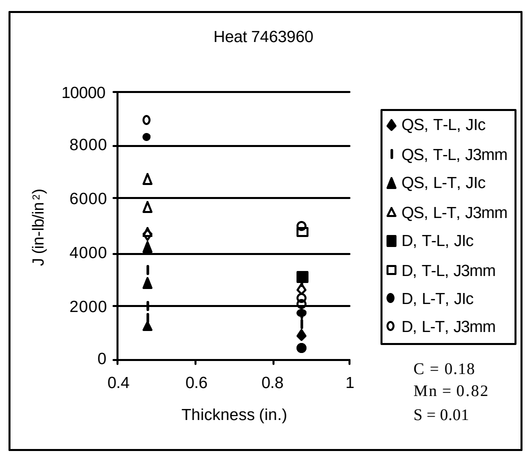

Figure 10: Fracture Toughness Response of Heat 7463960

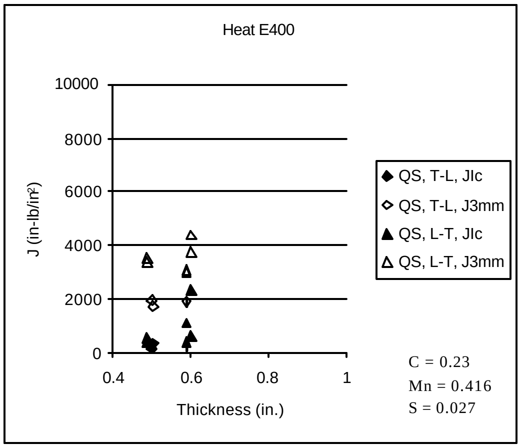

Figure 11: Fracture Toughness Response of Heat E400

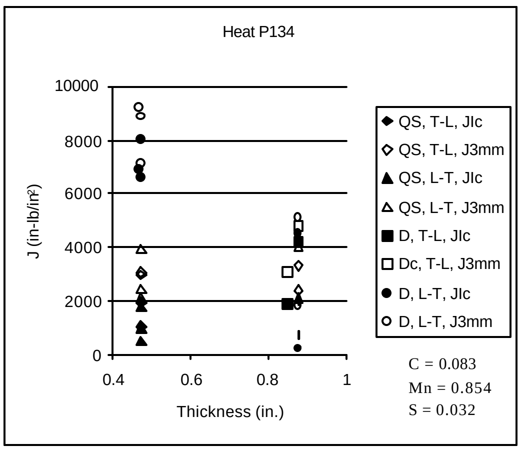

Figure 12: Fracture Toughness Response of Heat P134

STATISTICAL ANALYSIS

Four statistical models resulting from the combinations of loading rate (quasi-static, dynamic) and orientation (T-L, L-T) were developed for each of the measures of fracture toughness (J_{ic} and J_{3mm}).

Candidate terms for each model included all terms in the full 2nd order response surface model that contains all linear, cross product and squared terms. Since the data structure do not allow for the estimation of all terms in the 2nd order response surface model, statistical selection criteria (forward selection, backward elimination and the stage-wise procedure) were used to determine which terms (if any) to include in the final statistical models. All statistical calculations and modeling were preformed using the JMP statistical software. The chemical composition of each plate (carbon, manganese, and sulfur content) thickness, grain size and pearlite fraction were used as independent variables in modeling the fracture toughness properties. The terms in each of the models selected from the regression results, and the percentage of variation explained (R^2) are shown in Table 6 for the dynamic strain rate and Table 7 for the quasi-static strain rate. The variable legend is as follows:

- C – Carbon Content (wt%)
- M – Manganese Content (wt%)
- S – Sulfur Content (wt%)
- M/C – Manganese/Carbon Ratio
- T – Thickness (in.)
- G – Grain Size (in.)
- T – Thickness (in.)

Table 6: Significant Terms for Models Developed at the Dynamic Strain Rate

	LT	**LT**	**TL(*)**	**TL(*)**
	J_{Ic}	**J_{3mm}**	**J_{Ic}**	**J_{3mm}**
	T	T	None	
	G			G
R^2	**73%**	**58%**	**0%**	**67%**
n	12	12	15	15

(*) One outlier deleted 1A434-1&2, J_{Ic}=8515, J_{3mm}=8754

Table 7: Significant Terms for Models Developed at the Quasi-static Strain Rate

	LT	**LT**	**TL**	**TL**
	$\log_{10}(J_{Ic})$	**$\log_{10}(J_{3mm})$**	**$\log_{10}(J_{Ic})$**	**$\log_{10}(J_{3mm})$**
	S	C	P	T
	M/C	S	C	G
	S^2	C^2	M	C
		S^2	S	M
			P*C	S
				T*G
				M^2
				S^2
R^2	**53%**	**81%**	**86%**	**91%**
n	29	29	29	29

The log base 10 was applied to the fracture toughness measurements for the quasi-static loading rate models resulting in some model simplification. The results were transformed back to the original units to obtain the predictions. An R^2= 1 indicates that the regression curve goes through all data points while an R^2= 0 indicated that none of the data variability is explained by the variables in the model. The models for dynamic loading tests and quasi-static loading-LT do not explain a great deal of variability (R^2 ranges from 0% to 73%). Although the models show significance of certain variables, the models may be of limited usefulness because of the uncertainty around the predictions.

The final statistical models for the dynamic loading rate and quasi-static loading rate are displayed in Table 8 and Table 9 respectively.

Table 8: Dynamic Loading Rate Models

Dynamic, L-T

J_{Ic} = 47371.1 - 12604T - 672.4G

J_{3mm}= 13424.1 – 11615.8T

Dynamic, T-L

J_{Ic} = No Regression, Normal Distribution with Mean = 2397, Std. Dev = 1375

J_{3mm}= 26606.4 – 441.2G

Table 9: Quasi-static Loading Rate Models

Quasi-static, L-T

$\log_{10}(J_{Ic}) = 2.156 + 108.84S + 0.082M/C – 3342.5S^2$

$\log_{10}(J_{3mm}) = 3.411 + 3.577C + 40.089S – 19.295C^2 – 1360.8S^2$

Quasi-static, T-L

$\log_{10}(J_{Ic}) = 9.691 – 0.528P – 36.195C + 0.655M – 30.956S + 2.834CP$

$\log_{10}(J_{3mm}) = 9.911 – 12.568T – 0.143G – 1.756C + 6.584M – 65.131S + 0.2419GT – 5.202M^2 + 1368.64S^2$

DISCUSSION

The statistical models provide insight to the influence of the variables on the fracture toughness response of ASTM A285 steel. Grain size and thickness were found to have an effect on the dynamic fracture toughness while compositional factors play a greater role in the quasi-static fracture toughness. This may be due to the slow crack growth rate that allows for sampling of local microstructural features. However, at the dynamic strain rate, the crack growth rate may be too high.

There are several shortcomings to the statistical models. The regression fit of the models may allow for interpolation of the fracture toughness response with reasonably low error, however, does not have the accuracy for extrapolation of the variables beyond the bounds of the test program. In addition, the figure of merit chosen at J_{3mm} has been chosen on the assumption that cleavage fracture is not possible when the applied stress intensity is less than this critical energy. However, the scatter and the premature intervention of cleavage fracture of low carbon steel has led to the development of statistical and probabilistic methods to determine material properties for use in flaw stability. The method used in this test program is deterministic rather than probabilistic in its treatment of fracture toughness. Further analysis of the models will be done to understand their relationship with microstructural features.

CONCLUSIONS

Fracture toughness and tensile testing were performed on ASTM Type A285 steels that span Type I and Type II HLW tank plate compositions. The full data set was used to construct analytical models to predict fracture properties as a function of material properties and operating conditions. The models can be used to disposition specific flaws in tank plates by providing plate specific mechanical properties, and thereby reduce unnecessary conservatism inherent in using lower bound properties.

The models have several key conclusions:

- Geometric variables such as grain size and specimen thickness are statistically significant on the dynamic strain rate fracture toughness response.
- Compositional variables are statistically significant on the quasi-static strain rate fracture toughness response.

Further analysis will be done to relate the significance of each of the terms to known effects of each of the parameters on the fracture toughness.

ACKNOWLEDGMENTS

The authors of this report thank Dr. A. P. Reynolds, Dr. Y. J. Chao and K. Miller at the University of South Carolina for their assistance in testing fracture toughness specimens and producing J-R curves in 1999. The authors also thank Prof. J J. Lewandowski and Chris Tuma of Case Western Reserve University assisted in testing of the fracture toughness specimens from 200-2002. The authors thank Tracy Murphy for technician support throughout the experimental program.

REFERENCES

1 Sindelar, R. L., Lam, P-S., Caskey, G. R., Woo, L. Y., “Flaw Stability in Mild Steel Tanks in the Upper Shelf Ductile Range – Part 1: Mechanical Properties,” Journal of Pressure Vessel Technology, Vol. 122, pp. 162-168, May 2000.

2 Hamel, F. B., “An Investigation of the Impact Properties of Vessel Steels,” Proc. Div. of Refining of American Petroleum Institute, 38 (3), 239, 1958.

3 American Society for Testing of Materials, “General Requirements for Steel Plates for Pressure Vessels,” A20, January 2002.

4 Subramanian, K. H., Duncan, A. J., Sindelar, R. L., “Fracture Toughness Properties of Savannah River Site Storage Tank ASTM A285 Low Carbon Steel,” ASME PVP, July 2002.

5 Shanmugam, P., Pathak, S. D., “Some Studies on the Impact Behavior of Banded Microalloyed Steel,” Technical Note, Engineering Fracture Mechanics, Vol. 53, No. 6, pp. 991-1005, 1996.

6 Burns, K. W., Pickering, F. B., “Deformation and Fracture of Ferrite-Pearlite Structures,” Journal of The Iron and Steel Institute, November 1964.

7 American Society for Testing of Materials, “Standard Test Method for Measurement of Fracture Toughness,” E1820, 2000.

8 Duncan, A. J., Subramanian, K. H., Sindelar, R. L., Miller, K., Reynolds, A. P., Chao, Y. J., “Development of Mechanical Properties Database of A285 Steel for Structural Analysis of Waste Tanks.” ASTM STP 1406, June 2000.